Available online at www.sciencedirect.com
SCIENCE DIRECT
Journal of the European Ceramic Society 26 (2006) 2381–2387
www.elsevier.com/locate/jeurceramsoc

Optimization of the ceramization process for the production of three-dimensional biomorphic porous SiC ceramics by chemical vapor infiltration (CVI)

Daniela Almeida Streitwieser, Nadja Popovska *, Helmut Gerhard

Lehrstuhl für Chemische Reaktionstechnik, Universität Erlangen-Nürnberg, Egerlandstrasse 3, D-91058 Erlangen, Germany

Received 8 December 2004; received in revised form 15 March 2005; accepted 26 March 2005
Available online 13 May 2005

Abstract

The ceramization process for the preparation of three-dimensional (3D) biomorphic porous SiC ceramics by chemical vapor infiltration (CVI) with methyltrichlorosilane/hydrogen mixture has been optimized in this work. As a first step, two alternative ceramization routes have been compared with each other with regard to composition, morphology and bending strength of the resulting ceramics using flat samples. Optimal ceramization route was found to be a three-step process including carbonization of the paper preforms, followed by chemical vapor infiltration with stoichiometric SiC layers and a final oxidation step, in which the residual carbon from the template (C_b) is burnt out of the ceramics. Based on these results 3D honeycomb structures have been ceramized. Prior to these experiments, a computational fluid dynamics simulation of the gas flow in the reactor and through the honeycomb structure has been performed with the software STAR-CD. As a result, homogeneously infiltrated three-dimensional structured SiC ceramics could be produced.

Keywords: Chemical vapour infiltration; Films; Porosity; Mechanical properties; SiC; Biomorphic ceramics

1. Introduction

Biomorphic ceramics are materials made by a transformation of biological preforms into a ceramic material. Different applications are promising for such materials, especially for SiC ceramics, because of their good performance, including high mechanical strength, thermal stability above 1000 °C, high thermal conductivity and chemical inertness towards acids and bases.[1–4] The main applications for SiC monolithic ceramics or coatings can be found in high performance materials in motors or turbine blades or for abrasive wear protection.[1] The combination of the hardness of SiC with the low density and high flexibility of the biological structures makes biomorphic ceramics a unique material.

Different processing technologies have been developed in recent years. The most investigated among them are liquid Si infiltration,[5–8] Si gas infiltration,[5,9,10] SiO vapor infiltration[9,11] and chemical vapor infiltration and reaction (CVI-R).[1,12–15]

In our previous paper[12] the processing of porous SiC ceramics from paper by CVI-R technique was investigated. The paper fibers were first converted into a biocarbon (C_b) template by carbonization. In a second step methyltrichlorosilane (MTS) in excess of hydrogen was infiltrated into the C_b-template by CVI at relatively low temperatures (850–950 °C), depositing a Si/SiC layer around each fiber. The reaction (R) between carbon and excess of Si to form additional SiC occurred during the subsequent thermal treatment. As carbon normally does not react with the Si completely, the residual carbon has to be burnt out in an additional oxidation step. The bending strength of the resulting ceramics with a porosity of 70–85% was in the range between 5 and 15 MPa.

* Corresponding author. Tel.: +49 9131 852 7428; fax: +49 9131 852 7421.
E-mail address: n.popovska@rzmail.uni-erlangen.de (N. Popovska).

0955-2219/$ – see front matter © 2005 Elsevier Ltd. All rights reserved.
doi:10.1016/j.jeurceramsoc.2005.03.259

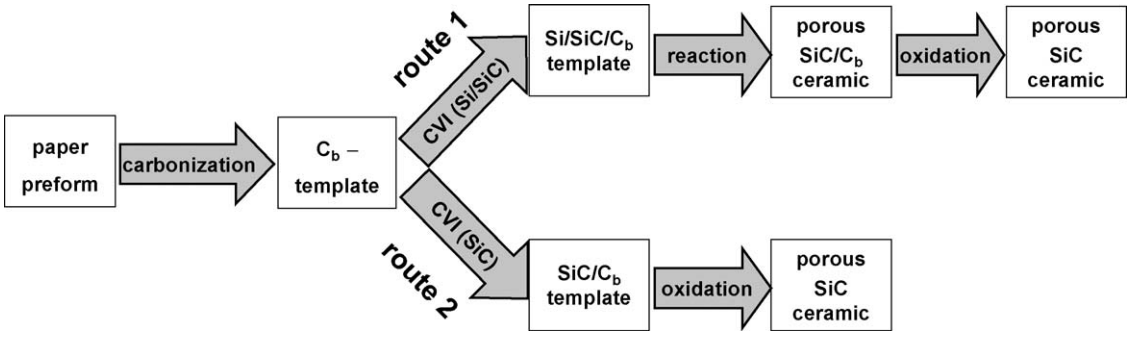

Fig. 1. Flow chart of the two routes of the ceramization process by CVI.

In this paper an alternative CVI ceramization route with the same precursor system (MTS/H_2) was investigated on flat substrates, shown as route 2 in Fig. 1. As in this case stoichiometric SiC is infiltrated, the carbon from the template remains unreacted and has to be burnt out in the last processing step.

After thorough investigations we have to select that ceramization route (Fig. 1), which produces ceramics with higher bending strength, for further use, in order to infiltrate three-dimensional (3D) structures. Previously, simulations of the gas flow in the reactor were performed with the computational fluid dynamics software STAR-CD.[16] By these simulations the distribution of the gas along the three-dimensional structures during the infiltration was analyzed in order to achieve a homogeneous infiltration, which was confirmed gravimetrically and by SEM.

2. Experimental procedure

2.1. Substrates

Flat paper sheets (Hahnemuehle GmbH), consisting of a mixture of linters and soft wood fibers were used for the conversion to SiC ceramics.[1] The paper has a thickness of 0.30 mm, geometrical density of 0.35 g/cm^3, an initial porosity of 0.69 and a mean pore size of 7.6 μm. Considering the shrinkage of the structures during the carbonization step, the papers were cut to 40 mm × 40 mm squares and carbonized at the optimal conditions, described in refs. 1, 12.

Three-dimensional structures were prepared from the same thin paper sheets with a flat and a corrugated layer. The last one consists of so called A-flute with a depth of 2 mm. By wrapping the layers and fixing them with standard paper glue onto the flat paper the shape of the structure was maintained after the ceramization process. The diameter of the 3D structures was set to 32 mm, while the length was 120 mm.

2.2. Experimental equipment

The equipment used for ceramization of paper preforms and the carbonization conditions were described in detail elsewhere.[12]

The chemical vapor infiltration process was performed with methyltrichlorosilane (MTS)/hydrogen mixtures. Two different layer compositions were used for the infiltration of the C_b-templates. According to our previous investigations with this precursor system,[12] the layer composition varies as a function of the deposition temperature and the hydrogen excess, expressed as the H_2/MTS ratio (α). Basically, at high temperature and low α values, stoichiometric SiC layers are obtained, whereas at low temperature and high hydrogen excess, Si rich SiC layers are deposited. Stoichiometric SiC was deposited at 950 °C and $\alpha = 2$. Layers with a Si/C ratio of 3 were deposited at temperatures between 800 and 925 °C and α values above 10. The infiltration experiments were performed at a reduced pressure of 300 mbar in order to achieve better infiltration into the pores of the C_b-templates, especially in the case of three-dimensional honeycomb structures.

When via route 1 excess Si was infiltrated in addition to SiC, it had to react with the carbon in a further thermal treatment step. The thermal treatment was performed at 1400 °C for 1 h in inert gas atmosphere. The amount of residual carbon was determined by thermogravimetric analysis (TGA).

An oxidation step is necessary either when biomorphic ceramics are produced with stoichiometric SiC layers or in the case, when Si/SiC layers are infiltrated. In both cases the residual carbon was burnt out of the inner core of the ceramic at 750 °C for 5 h.

2.3. Characterization methods

Thermo gravimetric analysis (Simultan-Thermo-Analyse-Geraet STA 429 Firma Netzsch-Gerätebau GmbH) was used to obtain the weight change of the samples when submitted to 750 °C for 4 h in air flow (50 N l/h). By this method the residual carbon in the final ceramics can be determined as it oxidizes easily in air at temperatures above 400 °C. Therefore, the weight loss of the samples is proportional to the amount of unreacted carbon in the ceramic. The TGA is comparable to the final oxidation step in the ceramization route.

Scanning electron microscopy (SEM Phillips XL 30) was used for analyzing the surface morphology of the preforms after every processing step.

Finally, in order to be able to make a statement about the quality of the processed ceramics, their bending strength was determined by a double ring bending test according to DIN 52 292.[16] The samples were subjected to a bending strength in radial and tangential direction between two metallic rings. A scheme of the double ring bending test and the calculations are presented in refs. 1 and 12.

3. Results and discussion

3.1. Ceramization of flat paper preforms

Flat paper preforms have been converted into SiC ceramics by applying the procedures described above (Fig. 1). In the case of ceramization route 1, where Si/SiC layers have been deposited, a subsequent thermal treatment step is necessary so that Si can react with the carbon to SiC as shown in Eqs. (1) and (2). The global reaction for the infiltration with stoichiometric SiC layers (route 2) is shown in Eq. (3).

Route 1:

$$3CH_3SiCl_3 + 4H_2 \rightarrow \ SiC \ + \ 2Si \ + \ 2CH_4 + 9HCl \qquad (1)$$

$$Si \ + \ C_b \rightarrow \ SiC_b \qquad (2)$$

Route 2:

$$CH_3SiCl_3 \xrightarrow{H_2} SiC + 3HCl \qquad (3)$$

In the following, samples prepared by routes 1 and 2 have been analyzed by TGA and double ring bending test and their properties have been compared with each other. From this analysis the ceramization route with the better results will be selected.

The degree of conversion of C_b to SiC (X) after thermal treatment as defined in Eq. (4) is analyzed by TGA.

$$X = \frac{C_{\text{converted}}}{C_{\text{initial}}} = \frac{C_{\text{initial}} - C_{\text{residual}}}{C_{\text{initial}}} = 1 - \frac{C_{\text{residual}}}{C_{\text{initial}}} \qquad (4)$$

The weight loss is inverse proportional to the degree of conversion of the C_b to SiC, so the weight loss after TGA as a function of the weight gain after infiltration and thermal treatment is presented in Fig. 2a. Higher conversion of the C_b to SiC can be observed after the thermal treatment. However, no complete conversion of the C_b to SiC was achieved at low weight gains. The main reason for this behavior is that in the low weight gain region no sufficiently free Si is being deposited that can react with the C_b (low Si/C_b ratio). So the main limitation of the conversion in this case is not the thermal treatment, but the availability of free Si. Also the slow diffusion of the C or the Si through the formed SiC layer is an additional limitation for a complete conversion.

The maximal bending strength as a function of the porosity, measured by Hg-porosimetry, is presented in Fig. 2b. A clear difference can be seen in the bending strength of the samples infiltrated with stoichiometric SiC and those infiltrated with Si/SiC layer and subsequently thermally treated. A possible explanation for the lower bending strength of the samples ceramized by route 1 is a crack formation as a result of volume expansion due to the high temperature reaction between Si and C_b.

The morphology of the samples prepared by both routes before the last oxidation step is presented in Fig. 3. Fig. 3a shows ceramics infiltrated with a Si/SiC layer and thermally treated, while Fig. 3b shows ceramics infiltrated with stoichiometric SiC. A C_b core is observed in both ceramics, but the SiC layers look smoother than the one obtained from the infiltration by the route 1. This confirms the higher bending strength of the ceramics obtained with the stoichiometric SiC layers.

From the results presented above an optimal ceramization route can be proposed. The route 2, including infiltration of the C_b-templates with stoichiometric SiC with a subsequent oxidation step, results in high porous ceramics with better bending strength. This route does not involve a high temperature treatment step, which makes it more economic.

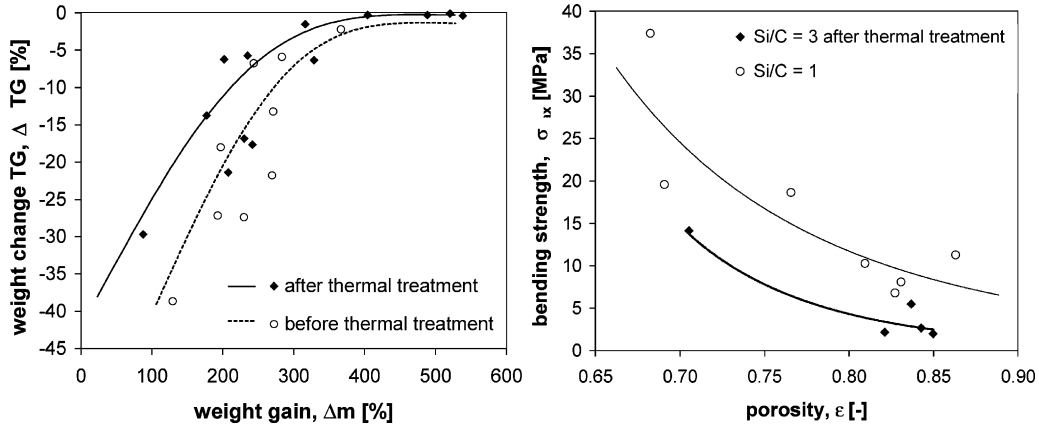

Fig. 2. (a) Weight loss during TGA and (b) maximal bending strength of the ceramics as a function of the thermal treatment step and the weight gain.

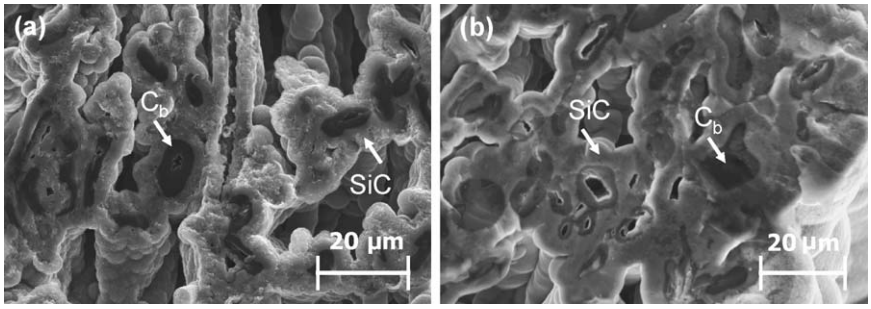

Fig. 3. SEM micrographs of samples infiltrated with (a) Si/SiC layer and (b) stoichiometric SiC layer.

3.2. Ceramization of three-dimensional (3D) structures

3.2.1. CFD simulation of the gas flow through the 3D structure

The gas flow during the CVI process of 3D structures has been simulated with the computational fluid dynamics (CFD) software STAR-CD.[17] For this study, first a grid for the reactor and the solid sample has been generated. The shape of the reactor tube with its inlet and outlet pipes has been modeled with a cylindrical coordinate system very similar to the actual equipment used. The reactor has a diameter of 32 mm with 130 cm length, while the furnace which is placed in the center of the tube has a length of 100 cm. The resistive heated furnace has been simulated by heating up the wall of the reactor with the measured temperature profile. The inlet and outlet pipes have a diameter of 7 mm. The inlet gas velocity in the pipe is set to 160 cm/s which correspond to a gas velocity in the reactor of 30 cm/s and a residence time of the gases of 2.0 s. The shape of the 3D structure has been modeled within the cell walls of the grid network. The same cells per square inch (cpsi) are set for the modeled structure as are obtained for the manufactured honeycomb structures, namely 145 cpsi. The structure walls are defined as baffles with a porosity of 0.50. So the gas flow is forced to pass along the whole length of the cells, but due to the porosity of the templates also some lateral diffusion through the cell walls is possible. In Fig. 4, the positioning of the three-dimensional sample in the reactor and its shape are presented.

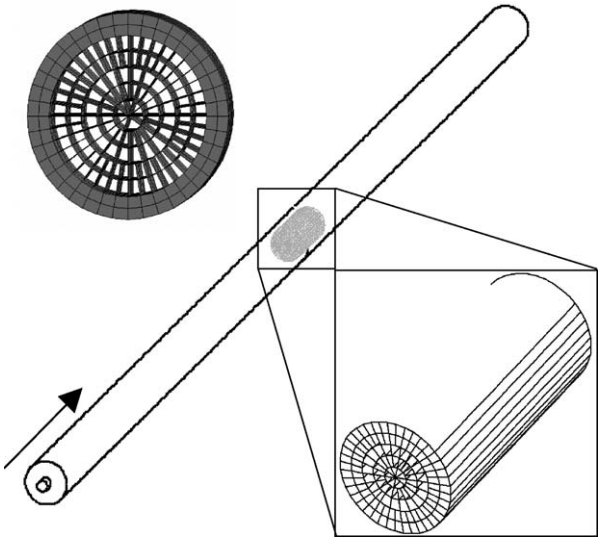

Fig. 4. Positioning of the 3D sample in the reactor.

In the simulation of the fluid dynamics the gas is entering the reactor through the inlet pipe and expands slightly, but a fast gas core remains until it reaches the samples. The gas mixes when passing through the 3D sample and thus, the gas

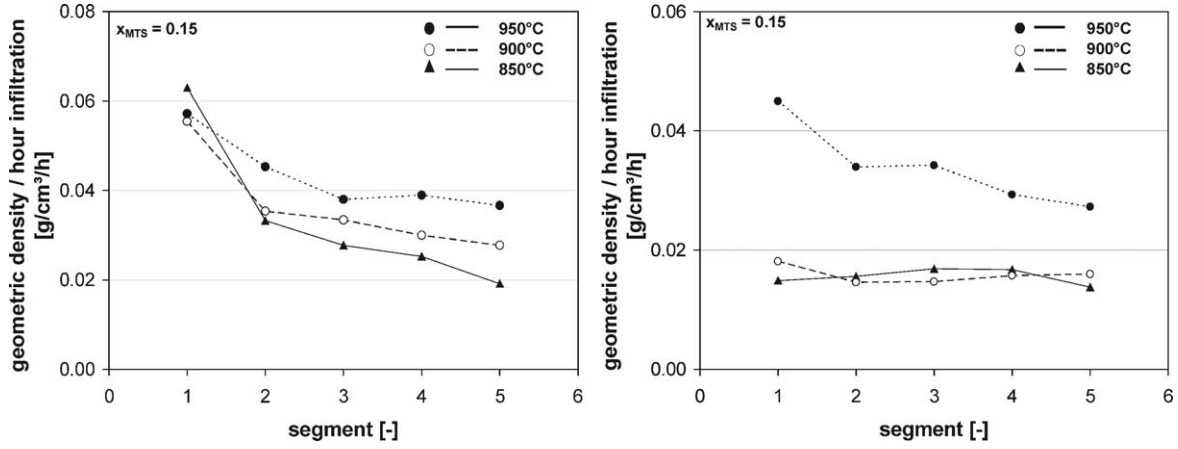

Fig. 5. Geometric density of the individual segments for different temperatures at (a) 300 mbar and (b) 100 mbar.

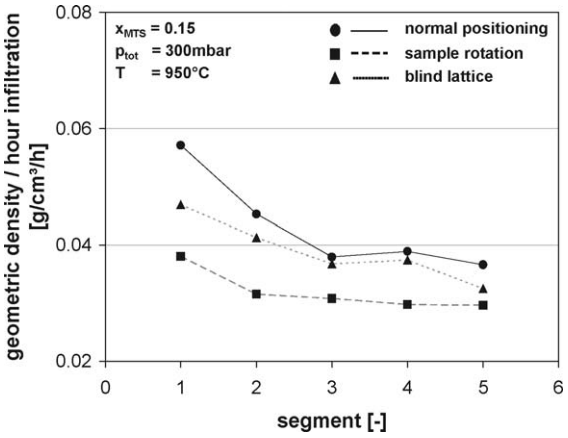

Fig. 6. Geometric density of the individual segments with alternative approaches: normal positioning (- - -) rotated samples and (· · ·) blind lattice.

velocity is more homogeneously distributed. This indicates that a good infiltration into the structure can be expected during the CVI process.

3.3. Ceramization of 3D structures

The 3D structures have been ceramized by the ceramization route 2, which includes carbonization, chemical vapor infiltration with stoichiometric SiC and a final burn out of the residual carbon by oxidation. The optimal parameters to obtain an axially homogeneously infiltrated structure must be determined experimentally. A clear effect of each infiltration parameter: temperature, total pressure and molar fraction of MTS (x_{MTS}) on the weight gain of the honeycomb structure was observed. In general, the weight gain increases with increasing the temperature, the total pressure and the molar fraction of MTS. However, the total weight gain does not give any information about the homogeneity of the infiltration within the 3D structures. Therefore, the homogeneity has been analyzed by cutting the samples in equal segments and calculating the geometric density of each segment. The principle is that the higher the geometric density, the higher the infiltration. An optimal infiltration is achieved at a high geometric density/h infiltration and homogeneous distribution along the individual segments. In Fig. 5, the geometric density for each segment at different infiltration conditions is presented. It can be clearly recognized that the overall values of the geometric density for the experiments at 300 mbar (a) is much higher than those for 100 mbar (b). Even if the distribution of the geometric density after infiltration at 100 mbar is more homogeneous than that at 300 mbar, the higher total pressure of 300 mbar will be applied for the following evaluations, because with experiments at 100 mbar more than 10 h infiltration is necessary to obtain the desired weight gain of at least 250%, which represent a geometric density of 0.18 g/cm^3. For the experiments at 300 mbar higher deposition rates are observed, especially at higher temperatures of 900–950 °C and a molar fraction of 0.30. However, a high difference in the geometric density of more than 60% was observed at these conditions between the first and the following segments of the 3D structures. Only for the second and the following segments, the geometric density was more or less constant.

In order to improve the homogeneity of the infiltration along the 3D structure, two approaches were investigated and

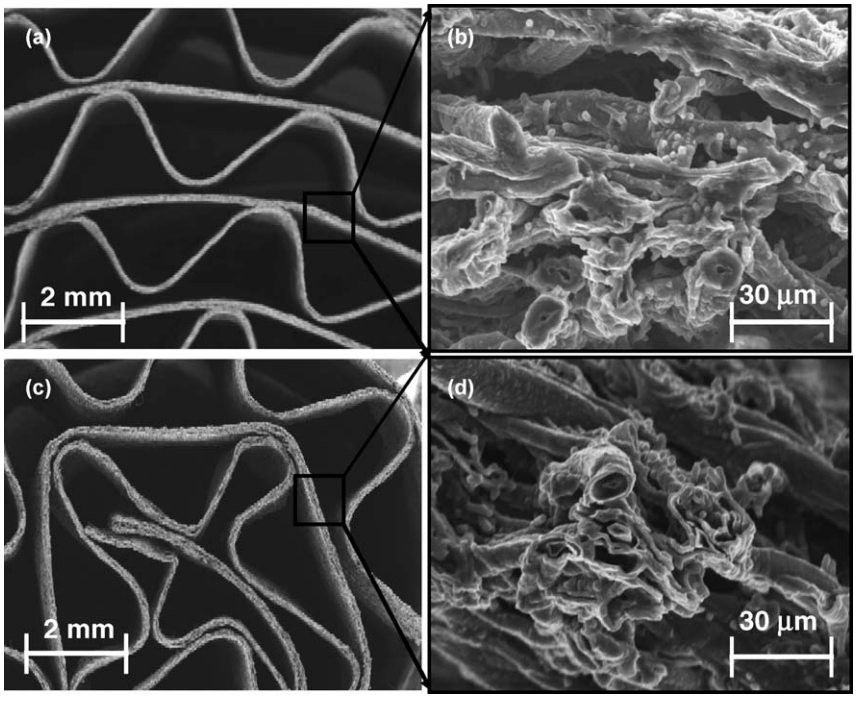

Fig. 7. SEM micrographs of the ceramized three-dimensional sample before (a and b) and after (c and d) oxidation.

presented in Fig. 6. The first curve (circles) shows the sample infiltrated at the optimal conditions at its normal positioning. In the second case (rectangles), the sample was taken out of the reactor after the half infiltration time and positioned again in the reactor the other way around. By rotating the samples, a more homogeneous infiltration can be expected, because both sides of the structure have been submitted to the same initial deposition rate. In the third approach (triangles), a thin 3D sample of 5 mm was prepared and placed in the front of the actual sample. This structure acts as a blind lattice, where the initially high deposition rate takes place. After that a more homogeneous infiltration along the complete length of the sample can be observed.

The results in Fig. 6 show that with both approaches a more homogeneous infiltration along the whole honeycomb structure was obtained. In order to simplify the process the approach of positioning a blind lattice before the actual sample was favored instead of rotating the sample. Two molar fractions of MTS have been investigated. At a molar fraction of 0.30 a high difference in the geometric density was still observed along the sample length, but at a molar fraction of 0.15 ceramized 3D structures with good homogeneity were produced. Therefore, the optimal infiltration conditions were set to 950 °C, 300 mbar, $x_{MTS} = 0.15$ and 5 h infiltration time with the blind lattice positioned directly before the sample.

In Fig. 7, SEM micrographs of two 3D structure segments are shown. This structure has been infiltrated at the optimal deposition conditions as indicated above. In Fig. 7a and b, the structure after the chemical vapor infiltration is presented, while in Fig. 7c and d the structure has already been submitted to the oxidation step for C_b removal. The fibers are hollow compared to the dense fibers of SiC with the C_b inner core before its burning out. No mechanical bending strength measurements can be performed with these structures due to their shape, but based on the results from the flat papers with the same weight gain in the range of 300–350%, bending strengths of a single wall between 10 and 15 MPa can be expected. And since the structure reinforces itself via the connections on the glued points, the real strength of the complete structure should be higher.

4. Conclusions

Biomorphic SiC ceramics have been prepared from flat and three-dimensional paper preforms by CVI with methyltrichlorosilane–hydrogen. As a first step the optimal ceramization route has been established using flat samples by analyzing the composition, the morphology and the bending strength of the ceramics, the last being the most important criterion. The optimal ceramization route was found to be a three-step process consisting of carbonization, chemical vapor infiltration with the deposition of stoichiometric SiC layers and a final oxidation, in order to remove residual C_b.

After defining the processing route, 3D structures were ceramized and characterized. Prior to the experiments a computational fluid dynamics simulation of the gas flow in the reactor and through the 3D structure has been performed. The results showed that a high velocity gas core remains, due to the thin inlet pipeline, up to the middle of the reactor until the sample is reached. But the gas flow homogenizes when it is passing through the 3D structure. Based on the simulation results a good infiltration can be expected.

Two approaches for further improving the homogeneity of the infiltration of the 3D samples were investigated and both were found to be effective. In the first case, the sample has been rotated in the reactor after half of the deposition time. In the second case, a blind lattice has been positioned before the 3D structure to homogenize the gas flow in front of the sample and also to obtain the maximum deposition rate in the blind lattice and therefore, more homogeneous deposition along the actual sample.

Acknowledgements

The authors thank the German Ministry of Education and Research (BMBF) for the financial support as part of the program: Development of Biomorphic Ceramics for the Exhaust Gas Treatment (03N8018E).

References

1. Almeida Streitwieser, D. Kinetic investigation of the chemical vapor infiltration and reaction (CVI-R) process for the production of SiC and TiC biomorphic ceramics from paper performs, dissertation, University of Erlangen-Nuremberg, Erlangen, 2004.
2. Sone, H., Kaneko, T. and Miyakawa, N., In situ measurements and growth kinetics of silicon carbide chemical vapor deposition from methytrichlorosilane. *J. Cryst. Growth*, 2000, **219**(3), 245–252.
3. Ganz, M., Dorval, N., Lefebvre, M., Péalat, M., Loumagne, F. and Langlais, F., In situ optical analysis of the gas phase during the deposition of silicon carbide from methytrichlorosilane. *J. Electrochem. Soc.*, 1996, **143**(5), 1654–1661.
4. Papasouliotis, G. D. and Sotirchos, S. V., On the homogenous chemistry of the thermal decomposition of methyltrichlorosilane. *J. Electrochem. Soc.*, 1994, **141**(6), 1599–1611.
5. Sieber, H., Hoffmann, C., Kaindl, A. and Greil, P., Biomorphic cellular ceramics. *Adv. Eng. Mater.*, 2000, **2**(3), 105–109.
6. Sieber, H., Kaindl, A., Schwarze, D., Werner, J.-P. and Greil, P., Light weight cellular ceramics from biologically-derived preforms. *cfi/Ber. DKG*, 2000, **77**(1–2), 21–24.
7. Herzog, A., Vogt, U., Graule, T., Zimmermann, T., Sell, J., Characterization of the pore structure of biomorphic cellular silicon carbide derived from wood by mercury porosimetry, ceramic materials and components for engines, Proceedings of the Seventh International Symposium, Goslar, Germany, 2001, pp. 505–512.
8. Sieber, H., Friedrich, H., Kaindl, A. and Greil, P., *Crystallization od SiC on Biological Carbon Precoursers; Bioceramics: Materials and Applications III (Ceramics Transactions 110)*. The American Ceramic Society, 2000, pp. 81–92.
9. Sieber, H., Vogli, E. and Greil, P, Biomorphic SiC-ceramic manufactured by gas phase infiltration of pine wood. Proceedings of the 25th Annual Conference on Composites, Advanced Ceramics, Materials, and Structures: B. *Ceram. Eng. Sci. Proc.*, 2001, **22**(4), 109–116.

10. Vogli, E., Sieber, H. and Greil, P., Biomorphic SiC-ceramics prepared by Si-vapor phase infiltration of wood. *J. Eur. Ceram. Soc.*, 2002, **22**, 2663–2668.
11. Vogli, E., Mukerji, J., Hoffmann, C., Kladny, R., Sieber, H. and Greil, P., Conversion of oak to cellular silicon carbide by gas-phase reaction with silicon monoxide. *J. Am. Ceram. Soc.*, 2001, **86**(6), 1236–1240.
12. Almeida Streitwieser, D., Popovska, N., Gerhard, H. and Emig, G., Application of the chemical vapor infiltration-reaction (CVI-R) technique for the preparation of high porous biomorphic SiC ceramics derived from paper. *J. Eur. Ceram. Soc.*, 2005, **25**(6), 817–828.
13. Sieber, H., Vogli, E., Müller, F., Greil, P., Popovska, N. and Gerhard, H., CVI-R gas phase processing of porous biomorphic SiC-ceramics. *Key Eng. Mater.*, 2001, **206–213**, 2013.
14. Greil, P., Vogli, E., Fey, T., Bezold, A., Popovska, N., Gerhard, H. *et al.*, Effect of microstructure on the fracture of biomorphous silicon carbide ceramics. *J. Eur. Ceram. Soc.*, 2002, **22**, 2697–2707.
15. Ohzawa, Y., Nakane, K., Gupta, V. and Nakajima, T., Preparation of SiC based cellular substrate by pressure-pulsed chemical vapor infiltration into honeycomb – shaped paper performs. *J. Mater. Sci.*, 2002, **37**, 2413–2419.
16. STAR-CD, version 3.15, Methodology, CD adapco Group, Computational Dynamics Limited, 2001.
17. DIN Norm 52 292 Teil 1, Bestimmung der Bruchfestigkeit: Doppelring-Biegeversuch an plattenförmigen Proben mit kleinen Prüfflächen, DK 666.151:620.174, April 1984.